

IMPACT OF DEPOSITION PROCEDURES ON 410L MULTILAYER PLASMA TRANSFERRED ARC PROCESSING

Otávio de Oliveira Lima^{1,2}

Gustavo Scheid Prass¹

Ana Sofia C. M. d'Oliveira¹

¹Federal University of Paraná, Department of Mechanical Engineering, Av. Cel. Francisco H. dos Santos, 100 – Jardim das Américas, Curitiba-PR, Brazil

²Volvo Construction Equipment North America, LLC, 304 Volvo Way, Shippensburg-PA, US

e-mails: otavio.lima@ufpr.br; gustavo.prass@ufpr.br; sofmat@ufpr.br

Abstract. Additive manufacturing (AM), Directed Energy Deposition (DED) technology is an important industrial manufacturing tool to produce mechanical parts without the use of expensive molds with functionalities otherwise not possible. AM can be carried out to fabricate new components or on maintenance of operations to rebuild the geometry of worn parts. Another benefit these manufacturing processes is the high efficiency use of material, increasing the competitiveness and reducing the carbon footprint of the process. Plasma Transferred Arc (PTA) is a low-cost, high-quality deposition technique that brings significant advantages in AM, and it was used to process multilayers of AISI410L. This study is part of an on-going study that addresses the impact of the deposition direction, bidirectional and unidirectional, and the mass flows (Q_m), 6 g/min and 9 g/min, on the solidification microstructure of multilayers. Walls were built using the four processing conditions and characterized in two different regions exposed to a larger and a small number of thermal cycles. Multilayers exhibited an epitaxial solidification structure with a growth direction that depended on the processing parameters used. Results pointed out that regions exposed to many thermal cycles, exhibited larger ferritic grains with an acicular structure at the grains boundaries and a uniform hardness varying between 180 HV and 200 HV. As the deposition height increased, the thermal cycles become smoother at the center of the multilayer walls. In contrast, the top region of multilayers exposed to a smaller number of thermal cycles revealed changes to the microstructure and hardness profile. The later exhibiting lower values at the last deposited layers varying between 150 HV and 185 HV (up to 5 thermal cycles) where larger grains formed followed by an increase up to 230 HV after 8 thermal cycles and the onset of the acicular structure. The low mass flow used allow for good finishing of the multilayers nevertheless the increase in mass flow resulted on an increase in hardness at the different regions and more significant changes at the top layers.

Keywords: Additive Manufacturing; Martensitic Stainless Steel; Plasma with Arc Transferred; Quenching and Tempering

1. INTRODUCTION

Technological advances available for the productive sector and its processes, added to the need for them to be increasingly sustainable, are considered a differential for companies operating in the manufacturing sector. Among the existing processes, the most used are casting and machining. The first presents a high cost due to the need to manufacture molds that are used only once or by high resistance molds for continuous use. In machining, either the conventional or CNC, the material removal process demands high energy consumption and generates a high amount of waste and, on some occasions, does not allow the production of parts with complex geometries.

Additive Manufacturing emerges as an innovative process that enables to manufacture parts and components with customized geometry, being able to offer complex geometries and with reduced costs when compared to conventional manufacturing processes through printing part by part, layer by layer until obtaining the final geometry defined in a 3D software (Thompson et al, 2016).

In this context, one of the benefits of AM stands out: the ability to use materials effectively, using the necessary amount for printing the component, reducing waste, and showing great relevance especially when working with materials that have a high-cost acquisition, considering the lowest need to subtract material (Pereira; Henke; D'Oliveira, 2018).

AM technology, particularly DED processes, allows to both designing and manufacturing parts directly from a digital file without the need of expensive tooling and the ability to add functionalities including structures with multiple materials. Within DED processes existing challenges and needs for the development of AM parts include planning the trajectory for the deposition of the desired part is highly relevant, however, the lack of solutions or alternatives for its optimization has been the subject of discussion for most of the problems related to the AM (Liu; To, 2017).

This investigation addresses this challenge assessing the impact of the deposition direction (bidirectional and unidirectional) and the powder-flow rate (6 g/min and 9 g/min) used on the microstructure and hardness of multilayers of atomized AISI 410L stainless steel.

2. MATERIALS AND METHODS

Multiple layers of gas atomized AISI 410L stainless steel powder (53-150 μm) were deposited using Plasma Transferred Arc (PTA) on AISI 304L substrate plates (L=150,0 mm, W= 12,7 mm, H=31,7mm) to obtain a 20 mm height multilayer wall. Four sets of processing parameters were used, Table 1, to assess the impact on microstructure and hardness depending on the processing conditions. The figure 1 shows the flowchart of multilayer deposition process and their characterization.

Table 1. Deposition parameters

Parameter	Value
Protective gas	Argon 99%
Plasma gas flow (l/min)	2.00
Shield gas flow (l/min)	15.00
Carrier gas flow (l/min)	0.80
Nozzle-plate distance (mm)	10
Deposition current (A)	150
Deposition speed (mm/min)	150
Powder flow rate (g/min)	6 and 9
Deposition direction	Bidirectional and Unidirectional
Deposition starting temperature between the multilayers	150°C

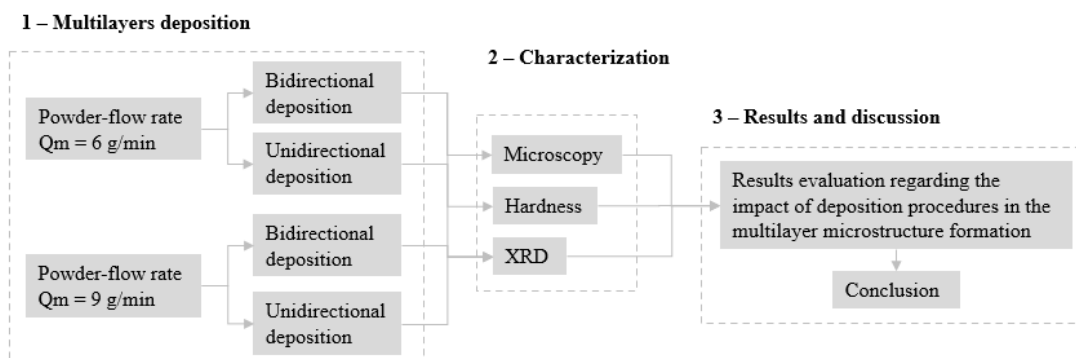


Figure 1. Flowchart of multilayer deposition process and their characterization

The figure 2 illustrates the deposition strategy according to the selected direction. An interlayer temperature was set at 150 °C, measured at the center of each deposited layer. During the bidirectional processing, from position A to B when the center region reaches 150°C the deposition of the second layer starts from position B to A, the procedure is repeated during the build-up of the multilayer wall. Similar procedure was used for the unidirectional processing except that in all layers deposition was carried out from position A to position B. The starting deposition temperature for bidirectional multilayers is higher than that of unidirectional multilayers because the deposition starting point was allowed more time to cool. Air-cooling to the interlayer temperature depended on the deposition strategy, with an average air-cooling time of 367 seconds for the bidirectional walls while for the unidirectional walls were 515 seconds.

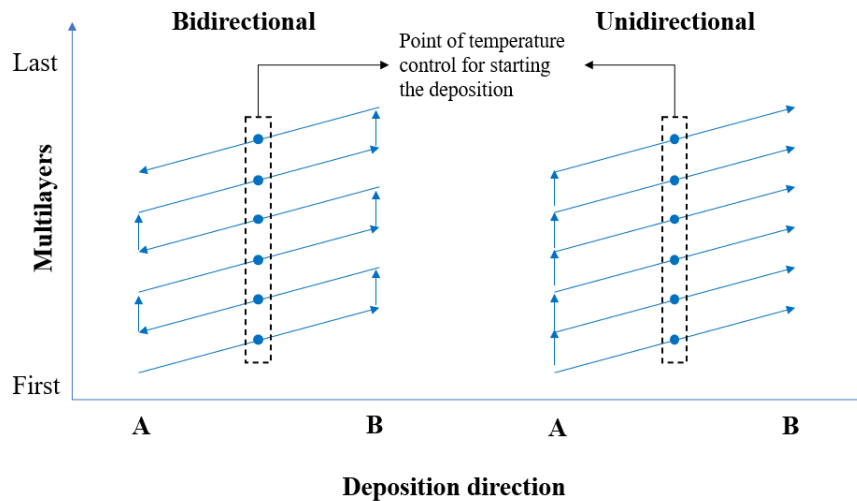


Figure 2. Deposition strategy

For the four set of processing conditions analysis was carried out at two regions associated with different thermal cycles: the center region which has a higher thermal cycles exposition, and the top region, exposed to a lower number of thermal cycles. Walls built with 6 g/min powder flow rate had a total 35 thermal cycles while the 9 g/min powder flow rate walls had 25 thermal cycles at maximum, with an average thickness of 0,65 mm and 0,98mm, respectively.

Five mm thickness samples were removed at the center of multilayer walls processed with the four set of parameters and embedded, followed by grinding with silicon carbide, and polished with 1 μm alumina. Polished samples were etched with Vilella reagent (10 ml of hydrochloric acid, 4 g of picric acid and 200 ml of alcohol) for 1 minute. The Vilella's reagent reveals the ferritic structure (α) etching the grain boundary (Carvalho Silva et al, 2005), the second phase particles (carbides, σ phase and δ ferrite) and reveals the martensite (Voort; Lucas; Manilova, 2004).

The hardness measurements were performed at the cross section of the samples in the center and top regions. For each region, measurements were made in a 5x3 matrix configuration, figure 3. On the top region, the upper measurements were taken 1.5 mm away from the surface and all indentations are 1 mm apart horizontally and vertically. The hardness measurements followed the ASTM E384/2017, Standard Test Method for Microindentation Hardness of Materials and the used parameters were: 10 N load and indentation time of 30 seconds.

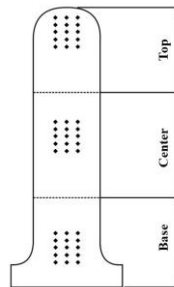


Figure 3. Hardness measurement matrix

The as-deposited multilayers underwent to X-ray diffraction analysis with 2θ interval between 40 and 120 degrees, scanning speed of 2 $^\circ/\text{min}$ and Cu tube. The results were analyzed with Chrystallografica Search-Match software.

3. RESULTS AND DISCUSSIONS

3.1 Deposition direction effects

The analysis of the thermal cycles in the processed multilayers for the two deposition directions used was carried out with the lowest mass flow rate tested, $Q_m = 6 \text{ g/min}$. The hardness profile for the multilayers processed with the two deposition directions, figure 4, shows that regardless of the deposition direction adopted, the same behavior is observed to the as-deposited condition.

Top regions of the multilayers show a significant variation in hardness. Near the top surface, exposed to up to 5 thermal cycles, the hardness varies between 155 HV and 185 HV, followed by an increase in hardness to 210 HV - 230 HV in the layers exposed to 8 or 9 thermal cycles. In contrast, in the center region of the multilayers, exposed to up to 25 thermal cycles, hardness exhibit more uniform values varying between 180 HV and 200 HV. Hardness profiles show that

at the top of the multilayers there is a volume of material that is strongly affected by the thermal cycle of the layer being deposited, and in regions far from the top, the volume of material exhibits uniform hardness, suggesting that the deposition temperature no longer induces significant transformations in the AISI410 stainless steel.

The last deposited layers exhibited a similar hardness profile a consequence of the solidification microstructure response to up to 7 heating and cooling cycles. However, walls processed with a unidirectional deposition strategy shifts the peak hardness to a smaller number of cycles also near the top of the wall hardness is lower compared to measurements made on near the top of wall build with a bidirectional scanning strategy. The observed differences in the hardness profile are associated with the starting deposition temperature of each layer and subsequent slower cooling rate measured for the unidirectional strategy.

The measured differences associated with the direction of deposition are reinforced by the work of Nikam, and Jain (2017) that mentioned that the temperature gradient for each multilayer deposited and the conditions for heat diffusion are better in the unidirectional deposition. The authors also observed that temperature gradient was constant after the deposition of the top five layers, reinforcing the measured hardness profile, figure 4. For the processing conditions used in our study peak hardness measured on the top region of multilayers is similar regardless of the deposition strategy as it is hardness measured at the center of multilayers.

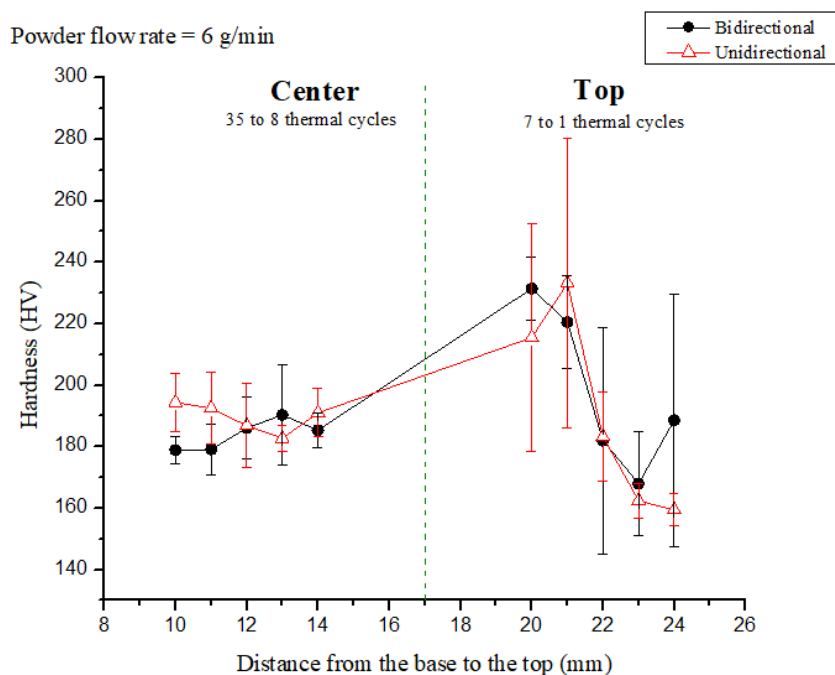


Figure 4. As-deposited multilayers hardness profile with 6 g/min of powder flow rate

The different deposition directions used to build the multilayer walls of AISI410 impact in the formation growth of the microstructure as represented in figure 5. The bidirectional deposition of multilayers induces a zigzag effect in the microstructure growth while unidirectional multilayer deposition is expected to impose the same growth orientation for each deposited layer of the processed wall. This behavior is not expected to be as pronounced as that observed in Powder Bed Melting (PBF) processes, which form a long and shallow melt pool that strongly affects grain orientation and structure (Dogu et al, 2022).

Epitaxial growth, which takes advantage of the crystalline orientation of the grains from the previous layer is observed from the first deposited layer in the multilayers regardless of the deposition directions. This phenomenon has also been described by Yehorov, da Silva and Scotti (2019) who also addressed microstructure growth with different deposition directions using wire of IN718. Parimi et al (2014) describe that in the unidirectional deposition columnar grains are smaller, and the growth direction exhibits an angle of less between 50° and 60°, while the bidirectional deposition results in angles between 90° and 100° relative to the substrate, and its inclination follows the back of the weld pool. The authors mention that this orientation could be related to the influence of vertical and horizontal heat flow, respectively, as well as the dendritic orientation of previously deposited layers.

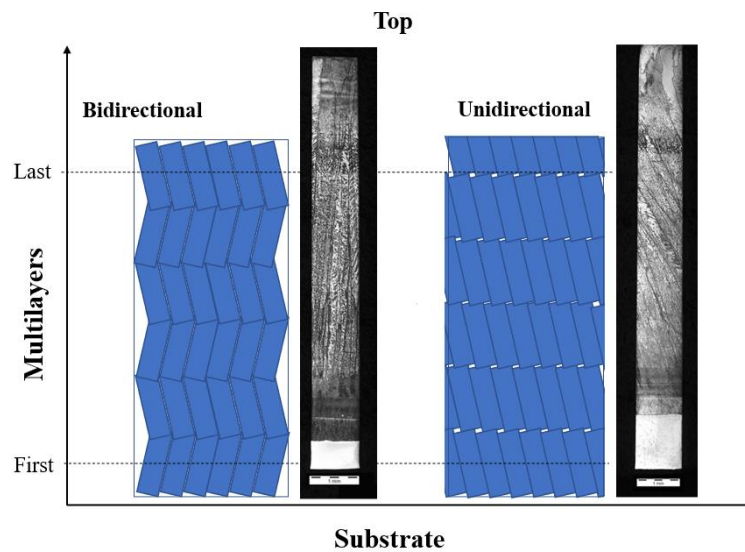


Figure 5. Effect of deposition direction on the microstructure of multilayers deposited by DED-PTA, as observed in the longitudinal section of processed walls

The thermal history that affected the measured hardness is also responsible for the microstructure of the multilayers. The figure 6 shows the longitudinal and transversal cross section of the microstructure of the multilayers processed with both bidirectional and unidirectional deposition strategy using 6 g/min as powder flow rate. It is observed that when the bidirectional deposition is adopted, it results in long columnar grains from the substrate to the top layers that in the cross section exhibit a radial growth orientation in relation to the substrate. In contrast, in the unidirectional deposition, grains at the transverse cross section are shorter corresponding to a section of the long columnar and incline grains observed in the longitudinal direction of the processed walls.

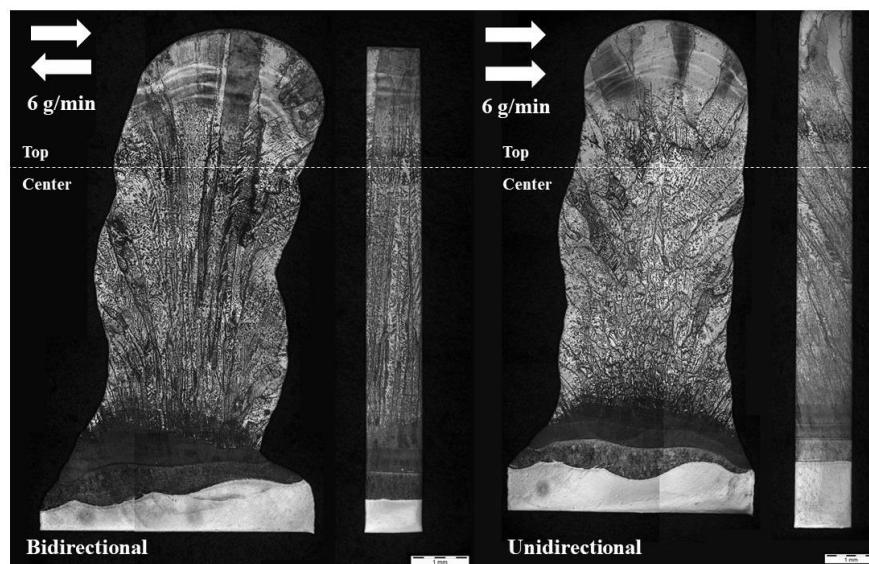


Figure 6. Bidirectional and Unidirectional walls microstructure deposited with 6 g/min powder flow rate

Regardless of the deposition direction, it is observed that epitaxial growth occurs during solidification in each deposited layer of the walls. This behavior is expected when layers of the same chemical composition and crystalline structure are deposited by welding processes, as cited by Alberti, Bueno and D'Oliveira (2015). In the top region, grain size is larger when compared to the center and base regions due to the high temperature at the top layers and smaller number of thermal cycles that were not enough to induce significant transformations in the solid state (Khodabakhshi et al 2020).

Figure 7 shows details of the microstructure for the as-deposited multilayers processed with 6 g/min in the bidirectional and unidirectional directions. Both processing conditions result in large grains covering the last 2-3 deposited layers exposed to more severe cooling-rate. For 410L steel, which has a high Cr/Ni ratio, it is expected that the first phase to solidify to be the δ ferrite and the high cooling rates associated with both PTA process and multilayer deposition induce

a greater ferrite formation, since the transformation in the solid state of ferrite into austenite takes less time to occur (Kou, 2003).

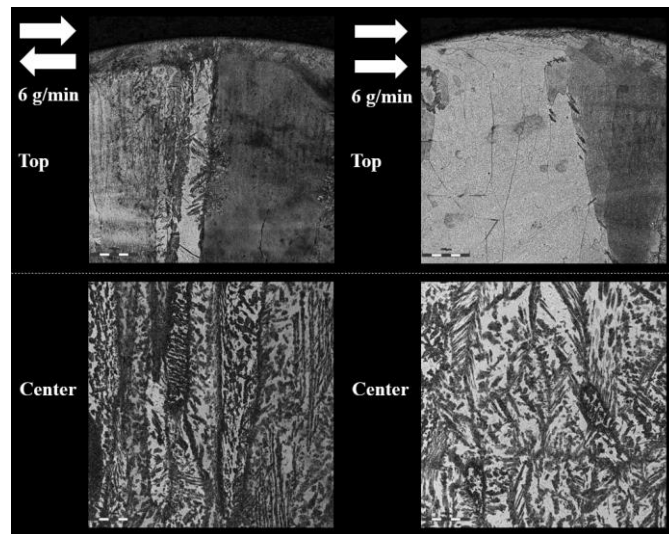


Figure 7. Cross-section microstructure detail for bidirectional and unidirectional depositions with 6 g/min powder flow rate with 500x enlargement

At the top of the multilayers an acicular structure forms at the grain boundaries identified as Widmanstatten austenite associated with the transformation in the solid state of ferrite \rightarrow austenite exposed to high cooling speeds. Kou (2003) also highlights the possibility of formation of either lacy or vermicular ferrite during the rapid solidification of steels with ferritic matrix, which is compatible with the observations made in the cross-section microstructure of the two deposition directions used.

For a better understanding of the transformations described above, it is necessary to point out that the martensitic and ferritic phases predicted by the Schaffler and DeLong diagrams for AISI410 steel, which agrees with the diffractogram made in the cross section, considering that the ferrite and martensite peaks are the same. This result can be associated with the cooling rates to which the multilayers were exposed, and the low carbon content of the steel used, AISI 410L.

Also, according to the Fe-Cr phase diagram and for the Cr content present in the alloy, the formation of austenite occurs after the formation of primary ferrite (δ). It is also relevant to highlight that, for alloys with low carbon content, the austenite loop is reduced, expanding the two-phase region, which tends to favor austenite, which will have Widmanstatten characteristics when cooled rapidly. The incoherent curved interfaces of the acicular phase have high mobility and allow the fast growth and continuous advancing on the ferrite. In the central region, exposed to the highest number of thermal cycles, a structure of ferritic grains and evidence of martensite are identified, as shown by the acicular structures that cut the grains transversally.

The figure 8 shows the detailed analysis of the X-ray diffractograms in the cross-section of the multilayers deposited with both bidirectional and unidirectional directions in the as-deposited condition with 6 g/min powder flow rate. It shows different displacements of the ferritic phase peaks, indicating differences caused by the deposition direction. Both walls showed an increase in their residual stress, displacement to the right of the peak of the reference chart (34-396), and that the unidirectional deposition direction induces a greater residual stress than the deposition in the bidirectional direction (Turibus, 2014). This difference may be related to the thermal cycles associated to each deposition direction. For unidirectional strategy deposition starts when the material is at a lower temperature when compared to that of bidirectional deposition, which facilitates the accommodation of stresses associated with solidification and the contraction and expansion of material already solidified from previous layers.

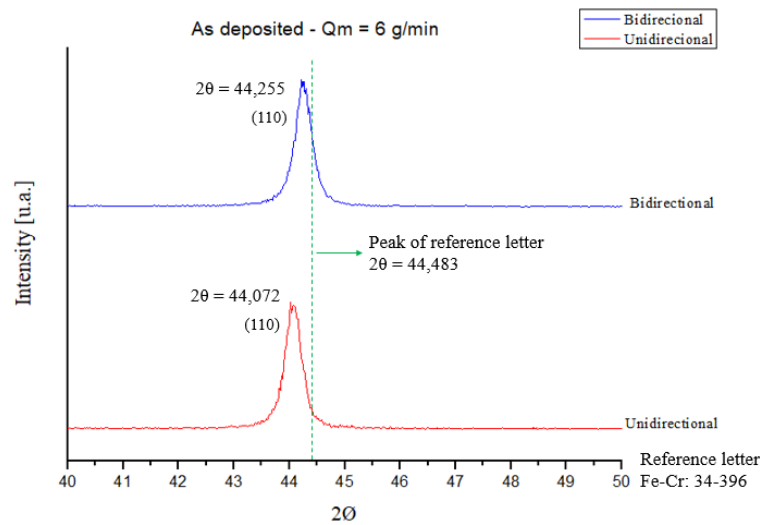


Figure 8. Detail of the diffractogram peak (110) for last deposited layer in both directions with 6 g/min powder flow rate

3.2 Impact of powder flow rate increasing in the multilayers

The immediate consequence of the powder flow rate increase is the deposition of thicker layers from 0.64 mm to 0.98 mm, and a smaller number of thermal cycles, for the same processed wall height. Despite the lower number of thermal cycles, the hardness profile remains similar except that the peak hardness at the top region is higher for the higher powder flow rate (9 g/min), figure 9.

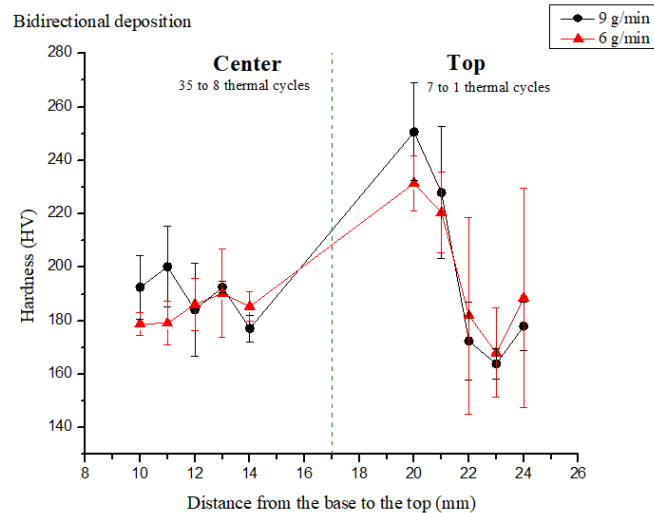


Figure 9. Hardness profile between the different powder flow rates for the multilayers with the bidirectional deposition

The temperature to which the material is exposed during multilayer deposition tends to decrease with increasing mass flow rate since more heat from the arc is absorbed to melt the material being deposited, and consequently, the time for air-cooling to the temperature of 150°C is expected to reduce.

Increasing the feeding rate to 9 g/min, did not change the major features imposed by the deposition strategy as shown in figure 5, but resulted in coarser structures figure 10. It is observed that the microstructure of these multilayers presents a similar characteristic to multilayers with 6 g/min, figure 6, epitaxial growth, grains with radial orientation in the bidirectional deposition and columnar grains in the unidirectional deposition when analyzed in cross section. It is also noted that, at the top region, the grains are larger when compared to the center region and have an acicular structure along the grain boundaries, identified as Widmanstatten austenite. With the higher feed rate, the material was exposed to a lower temperature and, therefore, it is observed that the primary ferrite grains are coarser when increasing the powder flow rate.

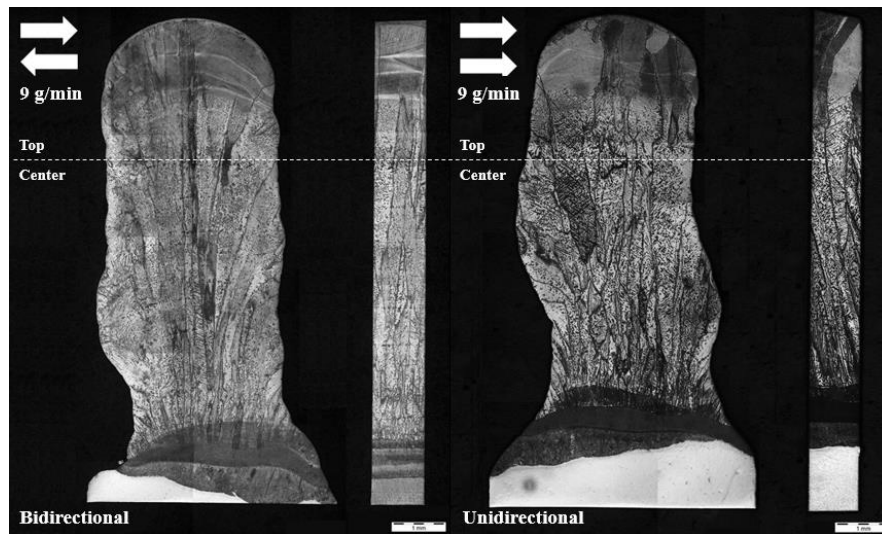


Figure 10. Bidirectional and Unidirectional walls microstructure deposited with 6 g/min powder flow rate

The figure 11 details the micrographs for the multilayers processed with 9 g/min in both bidirectional and unidirectional directions that have similar characteristics to Figure 7. It is also noted the presence of Widmanstatten austenite in the grain boundary and martensite in the central region of multilayers, between 8 and 35 thermal cycles.

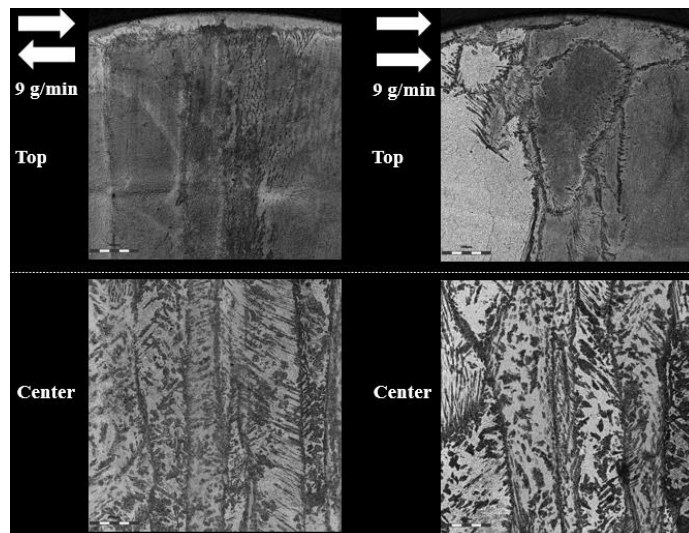


Figure 11. Cross-section microstructure detail for bidirectional and unidirectional depositions with 9 g/min powder flow rate with 500x enlargement

The X-ray diffraction for bidirectional and unidirectional deposition to the different powder flow rate used to build the multilayers walls are in the figure 12. As expected, the deposition direction and mass flow did not change the ferritic phase formed, as mentioned these peaks can be from either ferrite or martensite. Regardless of the deposition strategy multilayers compared to the smaller feeding rate, figure 8, there was a shift to the right and peaks are very similar to those of the reference chart (34-396).

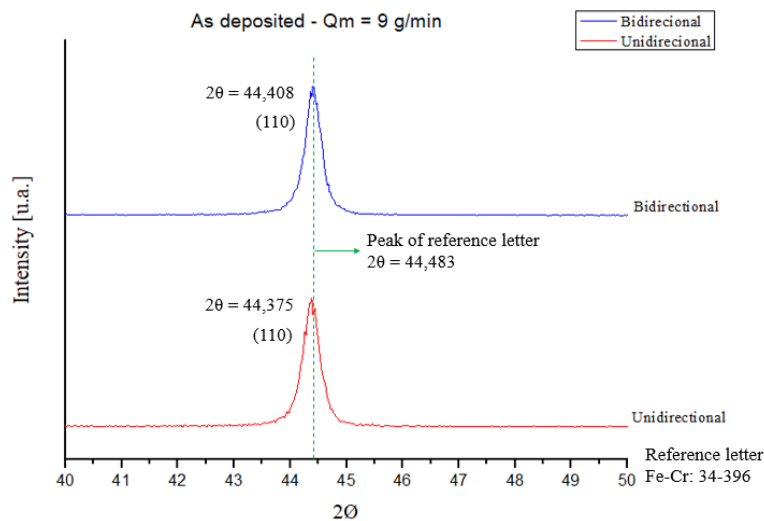


Figure 12. Detail of the diffractogram peak (110) for last deposited layer in both directions with 9 g/min powder flow rate

Results show that processing parameters induce changes in microstructure and hardness profiles of multilayers wall processed by PTA-DED that might remain after heat treatments. To mitigate the measured changes thermal management via mapping the impact of processing parameters can bring important benefits to multilayer processing reducing the need for expensive post heat treatment operations.

4. CONCLUSIONS

For the conditions tested in this investigation of the impact of deposition strategy and feeding rate on the features of multilayers of AISI 410 deposited by Plasma transferred arc PTA-DED, it is possible to conclude that:

Deposition strategy induces differences in the microstructure of multilayers characteristics because of different heat flow directions and cooling rates. Epitaxial growth occurs regardless of the processing parameters as confirmed by the long columnar grains at the longitudinal cross section of multilayers. At the transverse cross section of multilayers, bidirectional deposition strategy results in long columnar grains that extend from the bottom to the top layer whereas unidirectional deposition strategy accounts for the smaller grains.

Hardness profile is similar regardless of the processing parameters with a peak hardness near the top and a uniform hardness in the center; the slower cooling rates of unidirectional processing account for the peak hardness occurring closer to the surface

The increase in the powder flow rate resulted in thicker layers with a lower number of thermal cycles for the same wall height. This also modifies the behavior of the material and its microstructure in the top region, presenting larger and coarser ferrite grains.

5. ACKNOWLEDGEMENTS

The authors acknowledge, CNPq and the Laboratory of Additive Manufacturing and Surface Engineering (LAMSE) of UFPR.

6. REFERENCES

- Alberti, E. A.; Bueno, B. M. P.; D'Oliveira, A. S. C. M. Processamento de ligas de níquel com técnica de manufatura aditiva utilizando plasma por arco transferido. **Soldagem e Inspeção**, p. 137-147, 2015.
- ASM Handbook. Metallography and Microstructures. In: Voort, G. F. V; Lucas, G. M; Manilova, E. P. Metallography and Microstructures of Stainless Steels and Maraging Steels. **ASM International**, v. 9, p. 670-700, 2004
- Carvalho Silva, C.; Paulo Sampaio Eufrásio Machado, J.; Batista de Sant, H.; Pereira Farias, J. Estudo da sensitização causada pelo ciclo térmico de soldagem no aço inoxidável superferrítico AISI 444. **3º Congresso Brasileiro de P&D em Petróleo e Gás**, 2005.
- Dogu, M. N.; McCarthy, E.; McCann, R.; Mahato, V.; Caputo, A.; Bambach, M.; Ahad, I. U.; Brabazon, D. Digitisation of metal AM for part microstructure and property control. **International Journal of Material Forming**, 2022.
- Khodabakhshi, F.; Farshidianfar, M. H.; Gerlich, A. P.; Nosko, M Trembošová, V.; Khajepour, A. Effects of laser additive manufacturing on microstructure and crystallographic texture of austenitic and martensitic stainless steels. **Additive Manufacturing**, 2020.

Kou S. **Welding Metallurgy**, 2ª Edição, New Jersey, Editora Wiley; 2003.

Liu, J.; To, A. C. Deposition path planning-integrated structural topology optimization for 3D additive manufacturing subject to self-support constraint. **CAD Computer Aided Design**, v. 91, p. 27–45, 2017.

Nikam, S. H.; Jain, N. K. Three-dimensional thermal analysis of multi-layer metallic deposition by micro-plasma transferred arc process using finite element simulation. **Journal of Materials Processing Technology**, v. 249, p. 264–273, 2017.

Parimi, L. L.; Ravi, G.; Clark, D.; Attallah, M. M. Microstructural and texture development in direct laser fabricated IN718. **Materials Characterization**, v. 89, p. 102–111, 2014.

Pereira, H. C. B.; Henke, S. L.; D'Oliveira, A. S. C. M. IN625 multilayers characterization deposited by CMT. **Soldagem e Inspeção**, v 23, p. 235–246, 2018.

Thompson, M. K.; Moroni, G.; Vaneker, T.; Fadel, G.; Campbell, R. I.; Gibson, I.; Bernard, A.; Schulz, J.; Graf, P.; Ahuja, B.; & Martina, F. Design for Additive Manufacturing: Trends, opportunities, considerations, and constraints. **CIRP Annals - Manufacturing Technology**, v. 65(2), p. 737–760, 2016.

Turibus, Nolêto Sérgio. **Análise por difração de raios X do estado das tensões residuais em chapas de aço inoxidável duplex após soldagem**. 2014. 109 p. Tese de Doutorado (Engenharia Nuclear) – COPPE, Universidade Federal do Rio de Janeiro, Rio de Janeiro, 2014

Yehorov, Y.; da Silva, L. J.; Scotti, A. Exploring the use of switchback for mitigating homoepitaxial unidirectional grain growth and porosity in WAAM of aluminium alloys. **International Journal of Advanced Manufacturing Technology**, v. 104, p. 1581–1592, 2019.

7. RESPONSIBILITY NOTICE

The authors are the only ones responsible for the printed material included in this paper